SCIENTIFIC CULTURE

www.sci-cult.com

SCIENTIFIC CULTURE, Vol. 12, No. 1.1, (2026), pp. 5329-5342
Open Access. Online & Print

10.5281/zenodo.22648083

CATTANEO CRYSTOV EFFECT OF HYPERBOLIC TANGENT NANOFLUID FLOW OVER A STRETCHING SHEET

Kankanala Sharada[1*]

[1]Assistant Professor, Department of Mathematics, Chaitanya Bharathi Institute of Technology (A), Gandipet, Hyderabad, Telangana, 500075, Email: ksarada_maths@cbit.ac.in

Received: 27/11/2025
Accepted: 03/02/2026

Corresponding Author: Kankanala Sharada (ksarada_maths@cbit.ac.in)

ABSTRACT

The intension of the analysis is to scrutinize the two- dimensional darcy-forchheimer impermeable boundary layer hyperbolic tangent fluid flow beyond the bounds of a non-linear stretching sheet. Suitable similar variables are exercised to transmute the governing partial differential equations in to regular differential equations. Cattaneo Chrystov effect is introduced in this analysis. The outcomes of sundry variables on momentum, θ, ϕ are discussed.

KEYWORDS: Darcy-Forchheimer, incompressible, stretching sheet.

Copyright: © 2026. This is an open-access article distributed under the terms of the Creative Commons Attribution License. (https://cre-ativecommons.org/licenses/by/4.0/).

1. INTRODUCTION

Activation of motion procedure in porous space is complex due to the fluid and column wall and packing particles. Darcy's law is utilized to deliberate in tiny momentum suituations. It is analysed that Darcy's law mature insufficient for high velocity. Forchheimer [1] deliberates Darcy-Forchheimer constitution by including duel term of momentum in heat equation. Muskat [2] analised the Forchheimer factor.SureshKumar Raju et al. [3] ponders the impact of Darcy-Forchheimer flow and heat activation accreation of a viscoelastic fluid beyond a needle. Iftikhar Uddin et al. [4] illustrates the Darcy-Forchheimer behavior flow of Sisko fluid with nonlinear radiation.

M.U. Ahammad et al. [5] represents the wall stress and mass movement are exposed using graphs. Majeed et al. [6] illustrated 3 features. Initially, to articulate and inspect 2-D constitution for various fluids. Secondly to scrutinize the chemical reaction and another one, the duel order velocity slip condition are taken in to account. Srilakshmi et al. [7] elaborates the behaviour of Darcy-Forchheimer flow beyond the bounds of a stretching surface.Nanofluids accommodateminute nano sized particles. This outcome is prefer by Choi and Eastman [8] in 1995. Habib-olah Sayehvand and Amir Basiri pasra [9] have characterised the nano particles Impactforth electrical fluid by permeable medium. Rudraswamy and Gireesha [10] revealed their performance on the heat transport of nano-consistancy in the extanting of chemical effect. Rashidi et al. [11] have exposed the entropy fluid approach and take up to replicate the circumstance percularity condensation consists in stable solar. This fluid style is make use to deliberates the potential of nanoliquidbase fluid and to develope effective fertinity of a stable solar. The distinctive role of thermal radiation and the bio exert influence of heat process melting are bestowed in the flow of carbon nanotubes illustrated by Hayat et al. [12].Heat and mass flow of thermophoretic motion has potential utilizationsof nuclear reactor safety and microelectronics fabricant. The thermophoresis is reincarnation of sustained nanoparticles in a non-isothermal gas illustrates diminish a heat gradient and momentum is known as thermopheretic momentum.This abnormal consideration is illustrated by Das et al.[13].Ahmed et al.[14] illustrated the hyperbolic tangent nanofluid flow in hydro magnetic over a non-linear stretching sheet. Metib Alghamdi et al.[15] a special type of fluid (Eyring-Powell fluid) flows over a stretched cylinder, heated in two layers using a smart computing method to analyze the process. Noreen Sher Akbar et al.[16] how tiny particles (nanoparticles) spread in blood through a type of fluid flow in capillaries with a wavy membrane, influenced by electrical forces. Noreen Sher Akbar et al.[17] a process where a shear-thinning nanofluid (fluid with particles) is heated and created in a small, flexible channel with low fluid flow speed, using gold (Au) nanoparticles. Noreen Sher Akbar et al.[18] a study on improving heat storage and heat transfer using a hybrid Jeffrey nanofluid (a special fluid with nanoparticles) flowing through ducts with wave-like motion, while also looking at how energy is lost (entropy generation) in the process. Khalid Y. Ghailan et al. [19] studying how new nanoparticles interact with blood as they move through a porous channel, while considering the effects of energy and heat transfer during this process. Using a machine learning technique, Anum Shafiq et al. [20] demonstrated the significance of the bioconvective flow of an MHD thixotropic nanofluid via a vertical surface. Heat transfer enhancement in free convection flow of CNTs Maxwell nanofluids with four distinct kinds of molecular liquids was reported by Sidra Aman et al. [21].

Shafiq et al.[22] described , A dual stratification investigation on the stagnation point A statistical method for Walters' B nanofluid flow via a radiative Riga plate. MHD natural convection flow enclosure in a corrugated cavity filled with a porous media was demonstrated by Rizwan Ul Haq et al. [23]. Modelling Convective Transport in Al2O3-EO Mono-Nanofluid Around a Riga Wedge in Porous Media: A Hybrid Approach of Buongiorno's Law and Darcy–Forchheimer Theory Using Artificial Neural Networks was presented by Anum Shafiq et al. [24]. Darcy-Forchheimer magnetohydrodynamic Williamson nanofluid flow approaching a nonlinear radiative stretching surface was modelled by Shafiq et al. [25] using an artificial neural network.

2. MATHEMATICAL FORMULATION

The 2D impermeableover a non-linear extended plate, fluid flow in a boundary layer is presumptive. The fluid is hyperbolic at the tangent and forchheimer activation are also decided. We have presummated that the plate is extending quickly the velocity u=u_w=Bx^(1/3)beyond the boundsthe x-way, and the y-direction is perpendicular to the horizontal axis. A transverse magnetic field demonstrates the initiation of the flow. B^*=B_0/x^(1/3) vertically. Furthermore, the symbols C,T,T_w,C_w,T_∞,C_∞ mean, respectively, the concentration sketch, temperature sketch, wall temperature, wall concentration, ambient

temperature, and ambient concentration. The physical model of problem is illustrated in Fig.1.

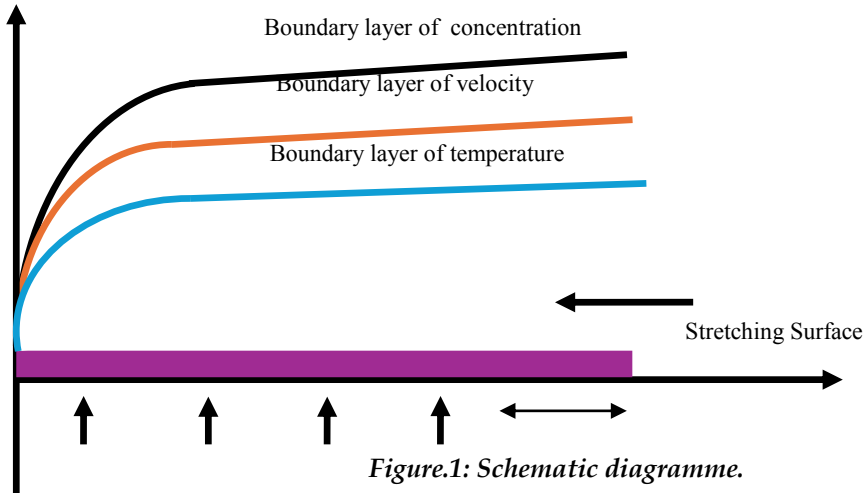


Figure.1: Schematic diagramme.

The following equations govern:

$\frac{\partial u}{\partial x}+\frac{\partial v}{\partial y}=0$ (1)

$u\frac{\partial u}{\partial x}+v\frac{\partial u}{\partial y}=\vartheta(1-n)\frac{\partial^2 u}{\partial y^2}+\sqrt{2\vartheta n}\Gamma\left(\frac{\partial u}{\partial y}\right)\frac{\partial^2 u}{\partial y^2}-\frac{\vartheta}{k}u-\frac{C_P}{\sqrt{K}}u^2+g\beta_T(T-T_\infty)+g\beta_C(C-C_\infty)$ (2)

$u\frac{\partial T}{\partial x}+v\frac{\partial T}{\partial y}=\frac{k}{\rho c_p}\frac{\partial^2 T}{\partial y^2}-\frac{1}{\rho C_P}\frac{\partial q_r}{\partial y}+\tau\left\{D_B\frac{\partial C}{\partial y}\frac{\partial T}{\partial y}+\frac{D_T}{T_\infty}\left(\frac{\partial T}{\partial y}\right)^2\right\}+$ (3)

$u\frac{\partial C}{\partial x}+v\frac{\partial C}{\partial y}=D_B\frac{\partial^2 c}{\partial y^2}+\left(\frac{D_T}{T_\infty}\right)\frac{\partial^2 T}{\partial y^2}-K_c(C-C_\infty)$ (4)

$u, v, \vartheta, \sigma, B_{0,} c, \rho, D_{B,} \alpha, T_\infty$ stands for density, specific heat, Brownian diffusivity, physical and electrical conductivity, magnetic field, kinematic viscosity, and ambient temperature.

The boundary conditions are

$u=u_w=Bx^{\frac{1}{3}}, v=0, T=T_w, C=C_w$ at y=0, (5)

$u\to 0, T\to 0. C\to 0$ as $y\to\infty$

To illuminate the governing constitutions are (2)-(4).

The similaritytransformations are

$u=Bx^{\frac{1}{3}}f'(\eta), v=-\frac{\sqrt{\vartheta B}}{3x^{\frac{1}{3}}}(2f(\eta)-\eta f'(\eta))$ (6)

$\left((1-n)+nWef''\right)f'''-\frac{f'^2}{3}-Krf'-Frf'^2+\lambda_1\theta+\lambda_2\phi=0$ (7)

$\theta''+\frac{2}{3}Prf\theta'+\frac{Nc}{Le}\phi'\theta'+\frac{Nc}{LeNb}\theta'^2=0$ (8)

$\phi''+\frac{2}{3}Scf\theta\phi'+\frac{1}{Nb}\theta''-Kr\phi=0$ (9)

After manipulating Eq (6) in Eq (5) the boundary circumferences reduced to Eq (10)

$f(0)=0, f'(0)=1, f'(\infty)\to 0$ (10)

$\theta(0)=1, \theta(\infty)=0, \phi(0)=1, \phi(\infty)=0$

$We=\sqrt{\frac{2B^3}{\gamma}}$ is utilized for weissenberg coefficient, $Pr=\frac{\vartheta}{\propto}$deliberates prandtl number , $Sc=\frac{\vartheta}{D_B}$represents Schmidt number, $Le=\frac{\propto}{D_B}$is the Lewis number, $Nb=\frac{D_B T_\infty(C_W-C_\infty)}{D_T(T_W-T_\infty)}$ represents diffusivity parameter , $Nc=\frac{\rho_p c_p}{\rho_c}(C_w-C_\infty)$ is heat capacity, $\lambda_1=g\beta_T T_0/a\vartheta$ and $\lambda_2=g\beta_C C_0/a\vartheta$ are temperature and concentration ratio coefficients , $Fr=\frac{C_p u}{\sqrt{k}}$ is darcy forchheimer,$Kr=\vartheta Kc(C-C_\infty)/u^2$is concentration parameter , $\beta_T=\frac{g\lambda_1(T-T_\infty)^2}{aB}$, $\beta_C=\frac{g\lambda_2(C-C_\infty)}{aB}$,

The Skin friction constitution (C_f), Nusselt number (Nu_x) and Shear wood number (Sh_x) are defined in equations (11) , (12),(13) given below

$C_f = \frac{\tau_w}{\rho u_w^2}$(11)

$Nu_x = \frac{x q_w}{(T_w - T_\infty)}$(12)

$Sh_x = \frac{x q_s}{(T_w - T_\infty)}$ (13)

Where $\tau_w = (1-n)\frac{\partial u}{\partial y} + \frac{n}{\sqrt{2}}(\frac{\partial u}{\partial y})^2{}_{y=0}$ (14)

$q_n = -(\frac{\partial T}{\partial y})_{y=0}$ (15)

$q_s = -(\frac{\partial C}{\partial y})_{y=0}$ (16)

Dimensionless forms of C_f,Nu_x and Sh_x are given in equation (11),(12),(13)

$Re_x C_f = \left((1-n) + \frac{}{2} wef''(0)\right) f''(0)$, $\frac{Nu_x}{Re_x} = -\theta'(0)$, $\frac{Sh_x}{Re_x} = -g'(0)$

3. NUMERICAL METHOD

This part presents the solution of the boundary conditions for ordinary differential equations (7)– (10) utilising the R-K shooting method. In order to accomplish this, first nonlinear differential constitutions must be solved into initial order linear equations. The following words refer to the components necessary for this law.

$$((1-n)+nwef^{"})f^{'''} - f^{'2} - krf^{'} + \lambda_1\theta + \lambda_2\theta + \lambda_2\phi = 0$$

$$\theta^{"} + \frac{2}{3}\Pr f\theta^{'} + \frac{N_c}{L_e}\phi^{'}\theta^{'} + \frac{N_c}{LeNb}\theta^{'2} + \delta_1\left(ff'\theta' + f\theta''\right) = 0$$

$$\phi^{"} + \frac{2}{3}Scf\theta\phi^{'} + \frac{1}{Nb}\theta^{"} - kr\phi = 0$$

$$f(0) = 0,\ f^{'}(0) = 1,\ f^{'}(\infty) \longrightarrow 0$$

$$\theta(0) = 1, \theta(\infty) = 0, \phi(0) = 1, \phi(\infty) = 0$$

$$f = f(1)$$

$$f^{'} = f(2)$$

$$f^{"} = f(3)$$

$$\theta = f(4)$$

$$\theta^{'} = f(5)$$

$$\phi = f(6)$$

$$\phi^{'} = f(7)$$

$$((1-n)+nwef^{"})f^{'''} = \frac{f^{'2}}{3} + krf^{'} + Frf^{1^2} - \lambda_1\theta - \lambda_2\phi$$

$$f^{'''} = \frac{1}{(1-n)+nwef^{"}}\left[\frac{f^{'2}}{3} + krf^{'} + Frf^{'2} - \lambda_1\theta - \lambda_2\phi\right]$$

$$f^{'''} = \left[\frac{1}{(1-n)+nwef(3)}\right]\left[\frac{[f(2)]^2}{3} + krf(2) + Fr\left(f(2)\right)^2 - \lambda_1 f(4) - \lambda_2 f(6)\right]$$

$$\theta^{"} = -\frac{2}{3}\Pr f(1)f(r) - \frac{Nc}{Le}f(7)f(5) - \frac{Nc}{LeNb}(f(5))^2 + \delta_1\left(f(1)f(2)f(5) + f(1)tw\right)$$

$$\phi^{"} = -\frac{2}{3}Scf(1)f(4)f(7) - \frac{1}{Nb}(t)\,fkrf(6)$$

$f_a(1)=0,\ f_a(2)=1,\ f_a(4)\longrightarrow 1,\ f_a(6)\longrightarrow 1,\ f_b(2)\longrightarrow 0,\ f_b(4)\longrightarrow 0,\ f_b(6)\longrightarrow 0$

4. RESULTS AND DISCUSSION

In this partition we deliberates the effecting of the participating constitutions on the f^',θ,φsketches as well as distributions of distinct relevant constitutions local Skinfriction , local Nusselt coefficient, Local Shearwood coefficient which are examined at the opening of graphs and tables.

Fig.2 illustrates the fluctuations in velocity portrait for different progressive valiues of ‘n’ deliberates the thickening performance of the fluid. In consideration of “n" is directly correlated with the fluid resistance rate in the fluids under discussion. There is a clear correlation between "n" and the fluid resistance rate. When taking the fluids into consideration. When a result, fluid resistance increases when 'n' improves and f^' (η) is lowered.Fig.3 deliberates the velocity portrait for various incremental values of inertial coefficient. We analysed with enhancing values of inertia coefficient (Fr). We also observed in Fig.3 illustrates diminishes the boundary layer. It can be utilized as a balancing mechanism. To delay the transition from the laminar boundary layer motion to turbulent motion. Fig.4 illustrates the diminishing trend. We carefully consider the fluid flow time scale to relaxation time ratio. Fig.5 reveals the temperature ratio coefficient. The outcomes of temperature ratio coefficient is enhanced then viscosity of fluids will be decreased. Fig.5 deliberates the enhancing trend. Concentration ratio coefficient effect is observed in Fig.6. Fig.6 illustrates the viscosity of fluids diminishing trend, when enhancing the concentration ratio coefficient. As Prandtl number Pr uplifted, the diminishes as illustrated in Fig.7. As the parandtl number Pr enhances, the thermal diffusivity becomes weaker as the kinematic viscosity boosting,the outcomes are higher fluid flow resistance. The exordinary Diffusion ratio effect Nb on is shown in Fig.8. So, by enhancing Nb , diminishes and the thickness of the thermal boundary layer shows the downward trend. The significance of heat capacity ratio Nc on is deliberates in Fig.9. Physically, in Nc on is illustrated in Fig.9. Physically, in Nc , particles expand other particles with a force that causes them to trancemigrate from a warmer to a colder region. Consequently, boosting the Nc result requires exerting extraordinary force on the other particles. Causing wider fluid to transmigrate. Fig.10 illustrates the Sc on concentration portrait. The impact of is diminished by enhancing the Sc. Sc is the ratio of velocity diffusivity to Brownian diffusivity, enhancing Sc induces a diminished in Brownian diffusivity, performing in a dull concentration portrait. The performance of Nb is illustrated in Fig.11. The decreasing trend is observed in Fig.11 portrait. The Nb values are enhancing the diminishing mode is observed in Fig.11. Fig.12 deliberates the Kr performance on concentration portrait. The outcome performance of Kr portrait deliberates the diminishing trend. Fig. 13 reveals the Skin friction coefficient on Pr. Pr values are increasing the enhancing trend is observed on Skin friction coefficient. Table 1 illustrates the comparision values of Skin friction coefficient at n=1,Fr=0,λ_1=0,λ_2=0,Kr=0

Table 1: Comparison values of $-f''(0)$ ***for We.***

We	Comparision table of Ahmed et al.[] (n=1, M=0)	Present
0.0	0.3191	0.3201
0.2	0.3182	0.3190
0.4	0.3172	0.3189

Table 2: Represents the various parameters effects on $-f''(0)$, $-\theta'(0)$ and $-$.

n	We	Kr	Fr	$_1$	$_2$	Pr	Nc	Le	Nb	Sc	$-f''(0)$	$-\theta'(0)$	$-$
0.1											0.9321	0.2097	0.6277

0.2											1.0166	0.2005	0.6101
0.3											1.0963	0.1897	0.6010
	0.1										0.9987	0.2210	0.5320
	0.2										0.9877	0.2190	0.5310
	0.3										0.9666	0.2010	0.5290
		0.1									1.1098	0.4567	0.7896
		0.2									1.0098	0.4365	0.7689
		0.3									0.9987	0.4273	0.7688
			0.1								0.8998	0.2343	0.8768
			0.2								0.8769	0.2234	0.8766
			0.3								0.8667	0.2132	0.8567
				0.1							0.9089	0.3452	0.6578
				0.2							0.9123	0.3899	0.6456
				0.3							0.9125	0.3900	0.6234
					0.1						1.0687	0.5478	0.2345
					0.2						1.0878	0.5520	0.2431
					0.3						1.0989	0.5674	0.2478
						1					0.9710	0.5320	0.2341
						2					0.9654	0.5230	0.2230
						3					0.9643	0.5210	0.2019
							0.5				0.8976	0.3421	0.2001
							0.6				0.7889	0.3342	0.1990
							0.7				0.7234	0.3120	0.1890
								0.1			0.3245	0.3456	0.3564
								0.2			0.3123	0.3342	0.3455
								0.3			0.2980	0.3212	0.3421

									0.1		0.7865	0.3321	0.2234
									0.2		0.7765	0.3421	0.2134
									0.3		0.7689	0.3456	0.2098
										0.1	0.8985	0.4325	0.3908
										0.2	0.8876	0.4216	0.2998
										0.3	0.8654	0.4132	0.2991

4. CONCLUSION

❖ The hyperbolic tangent flow of Darcy-Forchheimer across a non-linear expanding sheet is quantitatively examined in this work. The posteriors contain a list of this study's primary features.

- The velocity portraits of n, Fr, We diminished, $_1$, $_2$ portraits are enhanced.
- The temperature portraits of Pr, Nb are diminished, Nc portrait is increased.
- The concentration portraits of Sc, Nb, Kr are diminished.
- The values of n, $_1$, $_2$ are enhanced then $-f''(0)$ is enhanced.
- The values of $We, Kr, Pr, Nc, Le, Nb, Sc$ are enhanced the $-f''(0)$ is decreased.
- The values of Nb, $_1$, $_2$ are enhanced then $-\theta'(0)$ is increased.
- The values of $n, We, Kr, Pr, Nc, Le, Sc$ are enhanced the $-\theta'(0)$ is decreased.
- The values of $_2$ is enhanced then $-$ is enhanced.
- The values of $n, We, Kr, Pr, Nc, Nb, Le, Sc$ are enhanced then $-$ is diminished.

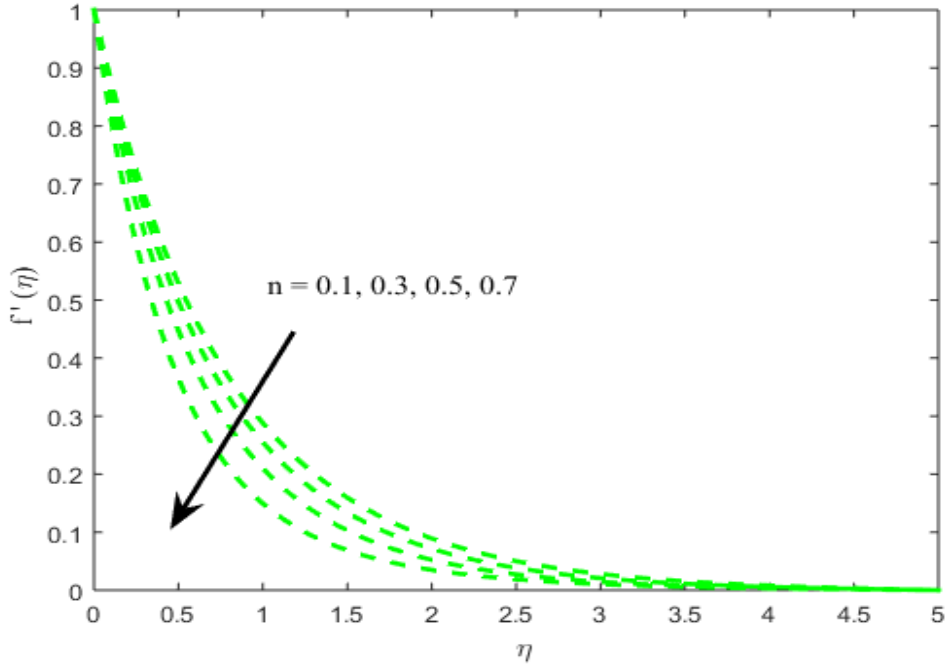


Fig.2 prominence of n on $f'(\eta)$

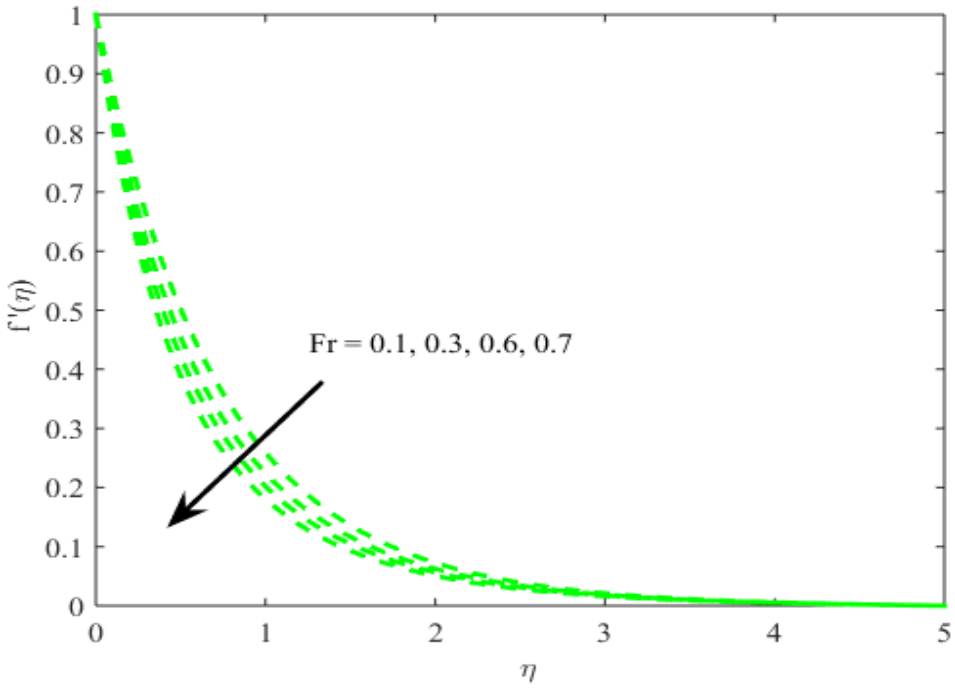


Fig.3 prominence on Fr on $f'(\eta)$

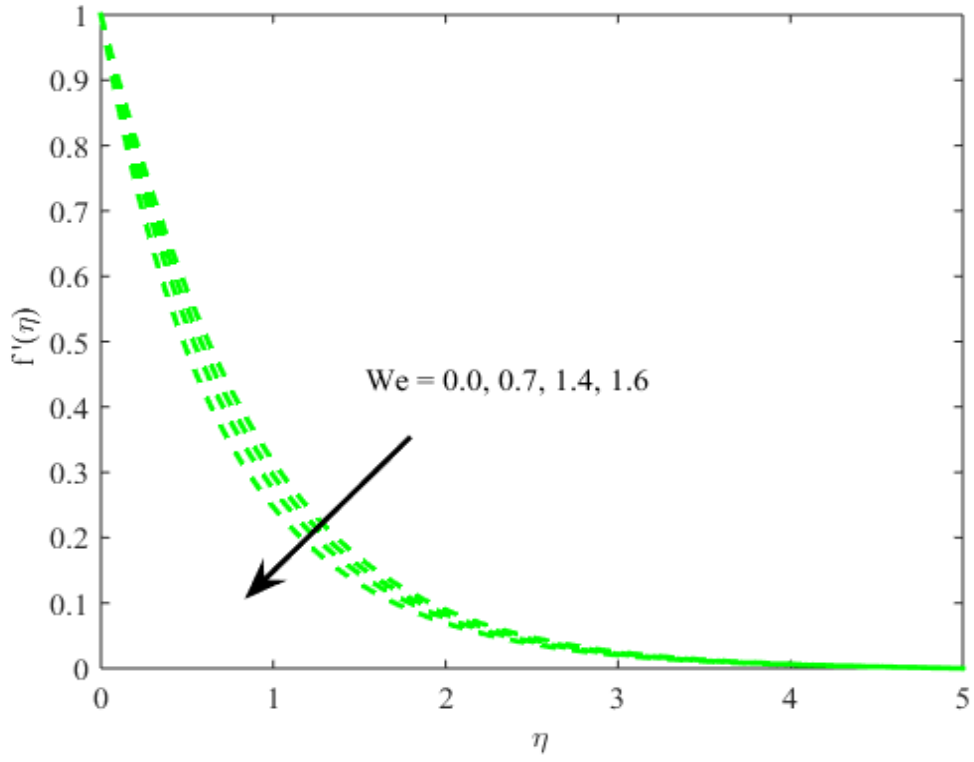


Fig. 4 prominence on We on $f'(\eta)$

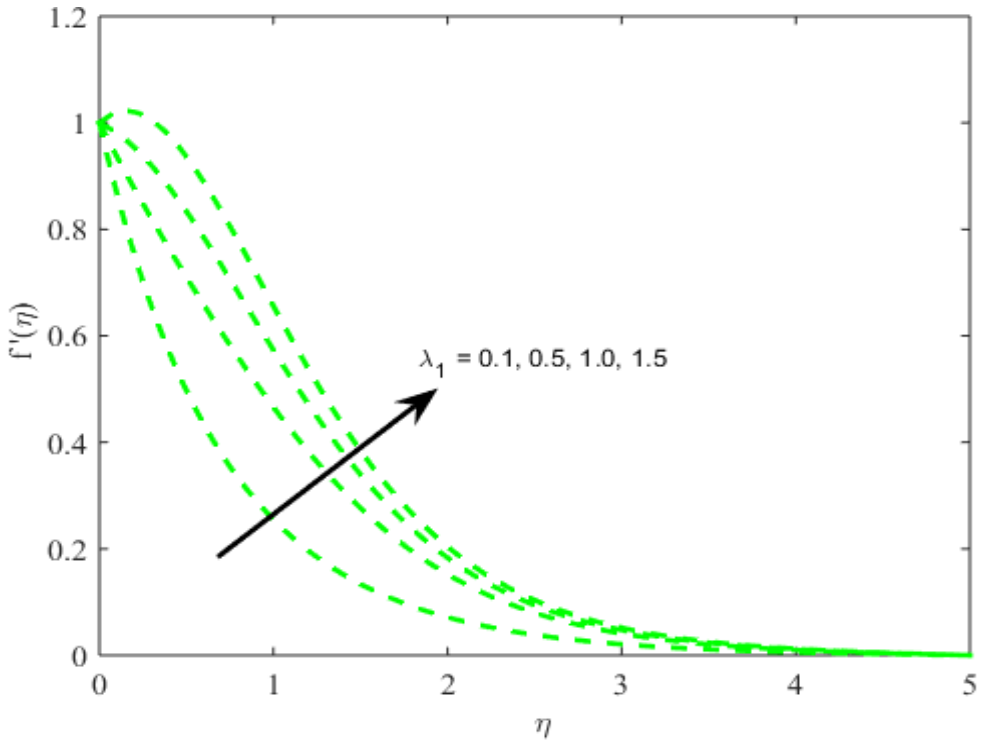


Fig.5 prominence on λ_1 on $f'(\eta)$

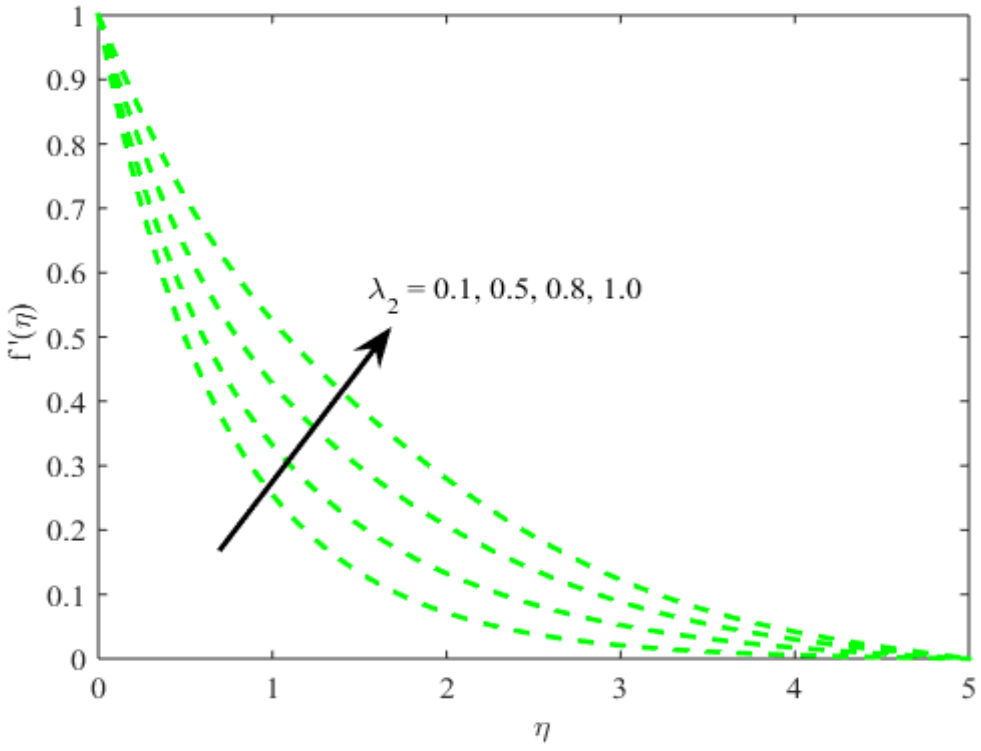


Fig.6prominence of λ_2 on $f'(\eta)$

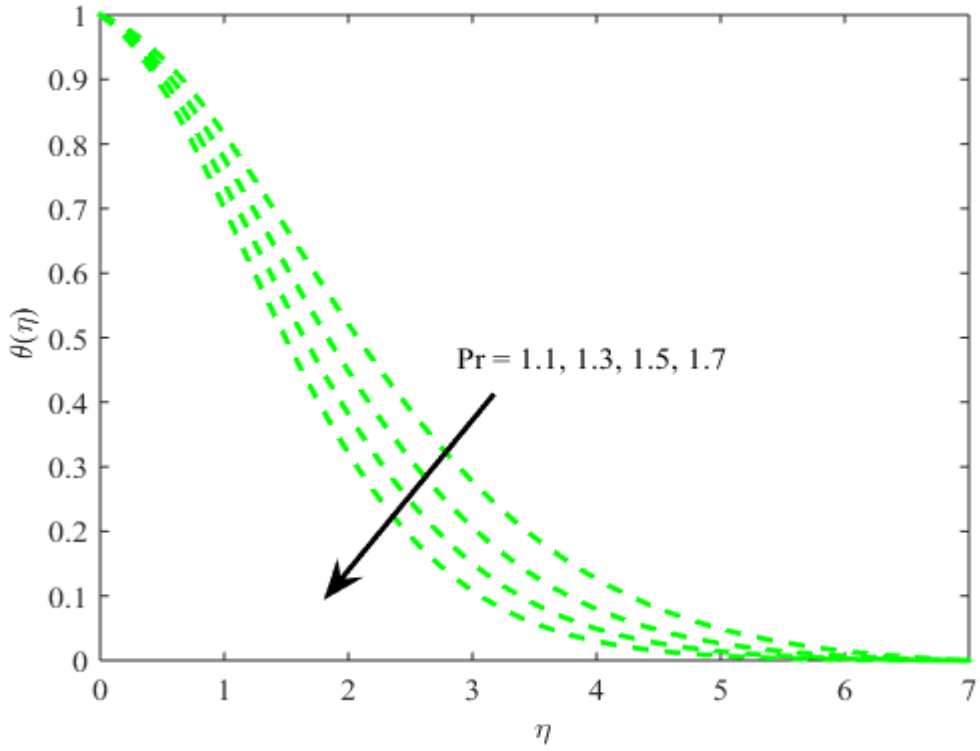


Fig.7 prominence of Pr on θ()

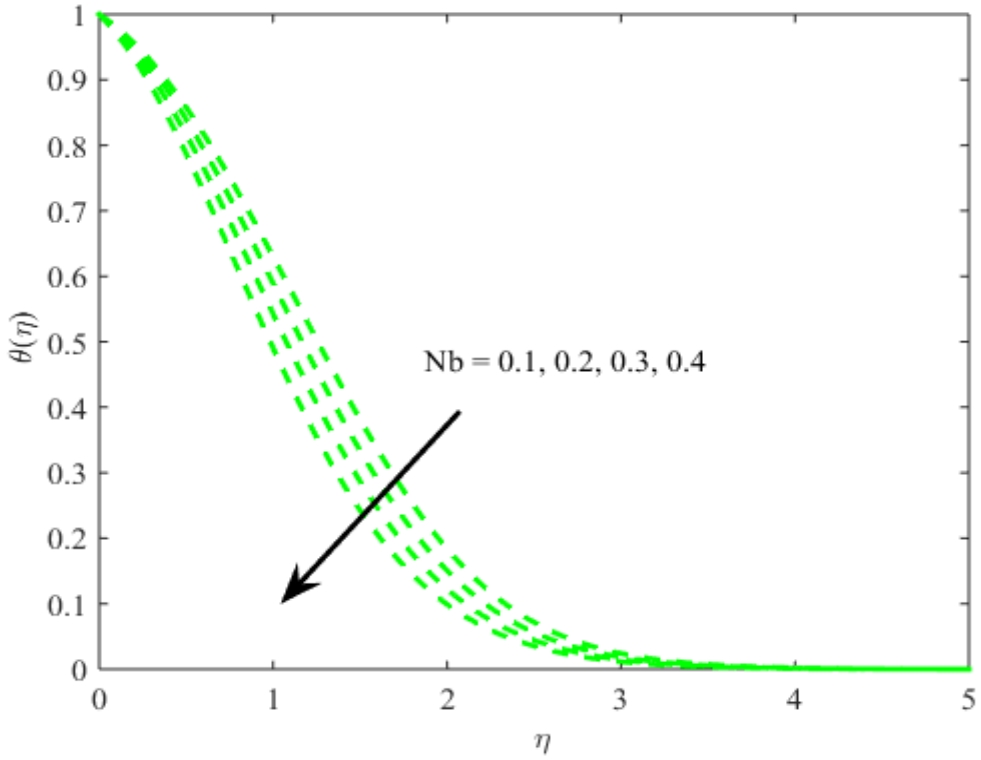


Fig.8 prominence of Nb on θ()

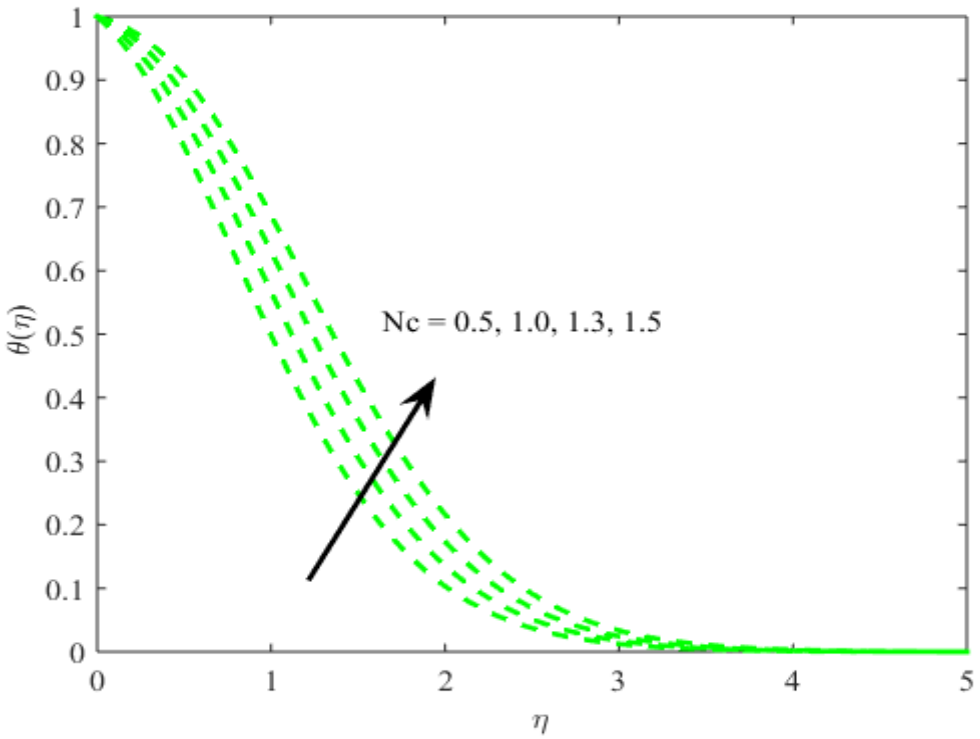


Fig.9prominence of Nc on $\theta()$

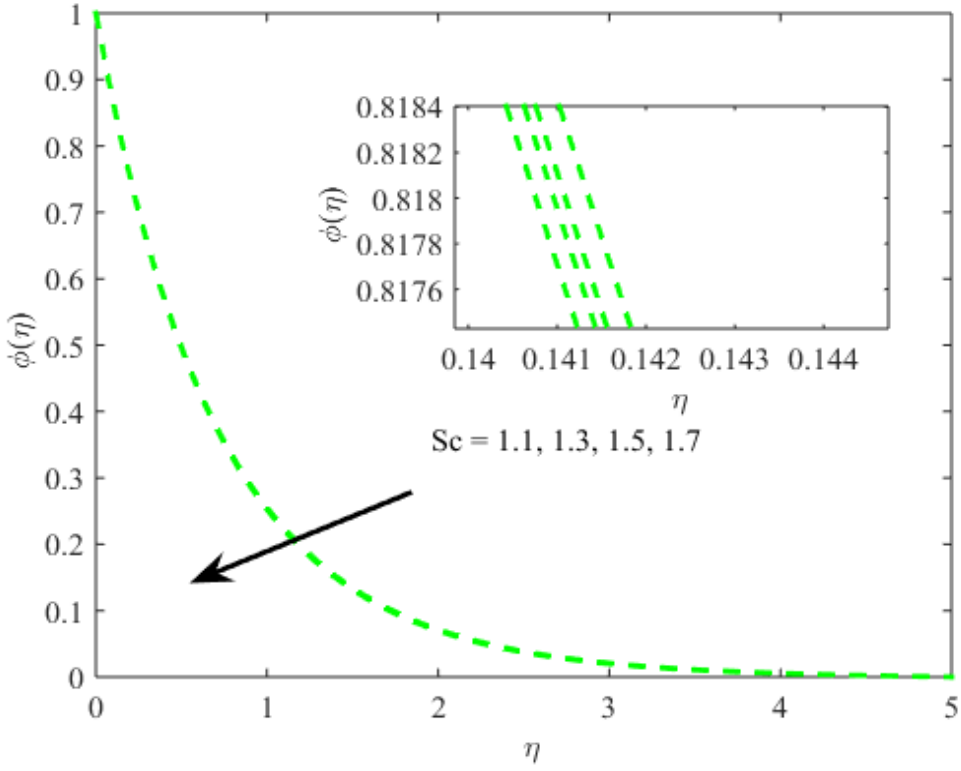


Fig.10 prominence of Sc on $\phi(\eta)$

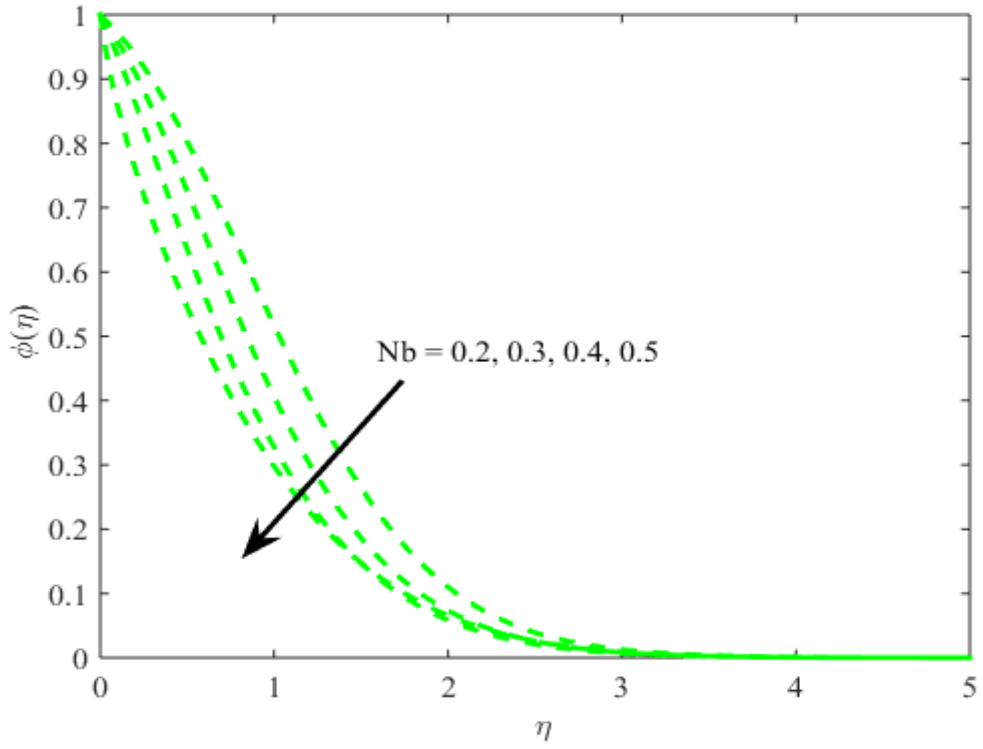


Figure.11: prominence of Nb on $\phi(\eta)$

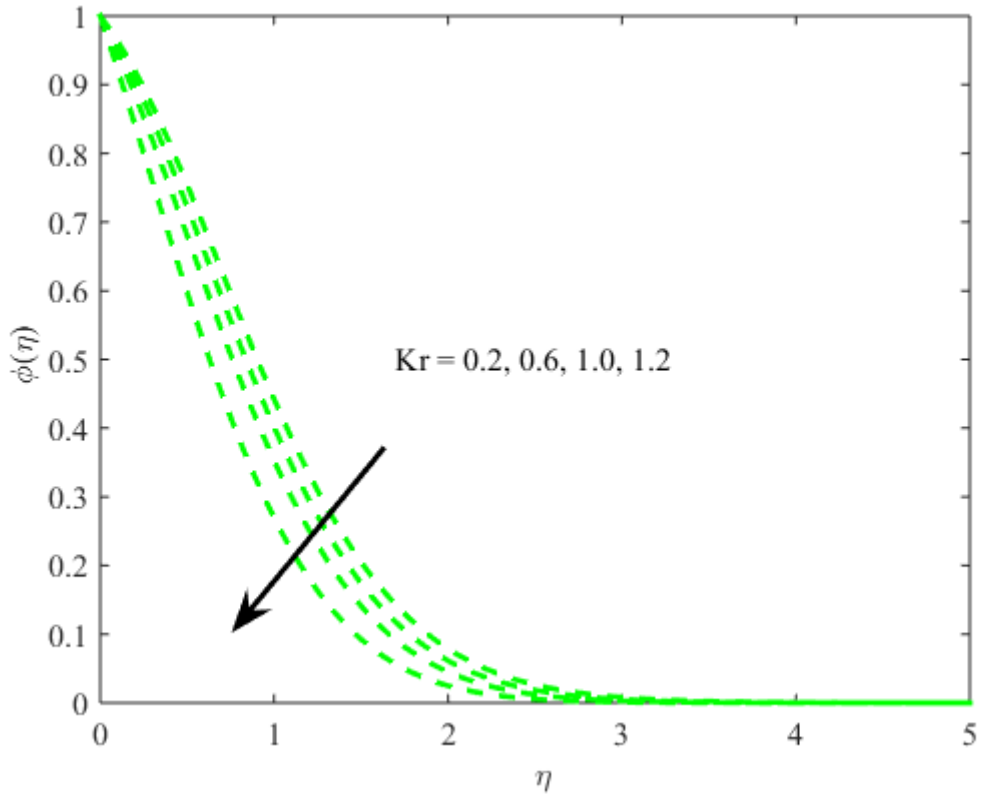


Figure.12: prominence of Kr on $\phi(\eta)$

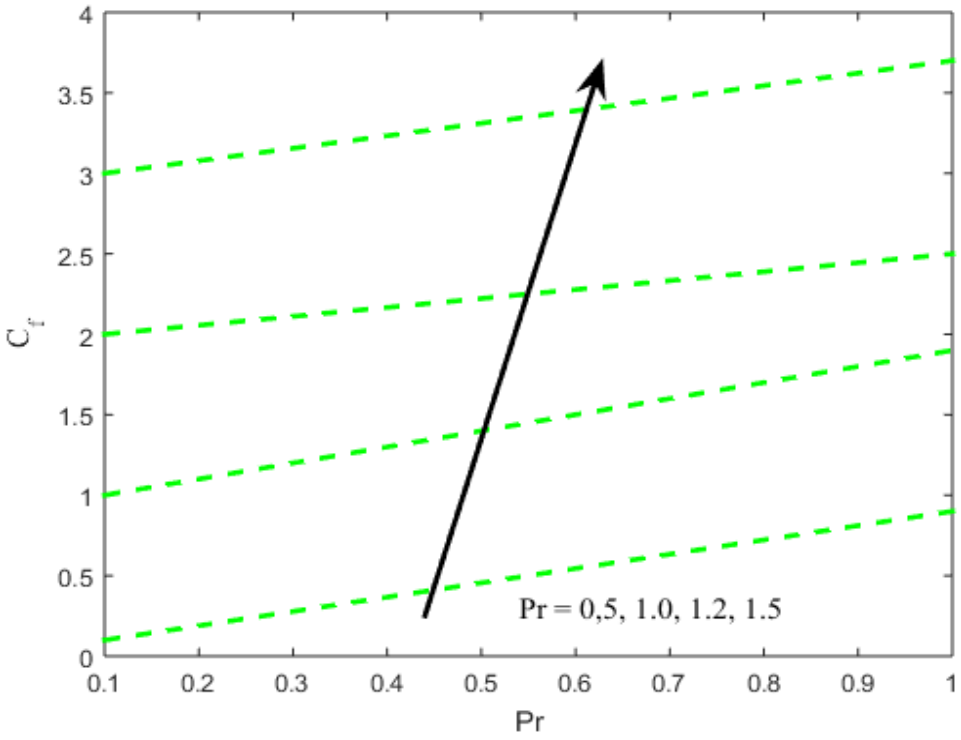


Figure.13: prominence of Pr on Skinfriction coefficient

REFERENCES

[1] Forchheimer. P, Wasserbewegung durch boden, Z ver D Ing, 1901, Vol.45, pp.1782-1788.

[2] Muskat.M, The flow of homogeneous fluids through porous media, Edwards, MI, 1946.

[3] Sureshkumar Raju S, K.Ganesh kumar, Mohammad Rahimi Gorji and IIyas khan, Darcy –Forchheimer flow and heat transfer augmentation of a viscoelastic fluid over an incessant moving needle in the presence of viscous dissipation, Microsystem technologies, (2019).

[4] Iftikhar Uddin, Rizwan Akhtar, Zhuzhiyu, Saeed Islam, Muhammad Shoaib and Muhammad Asif Zahoor Raja, Numerical treatment for Darcy-Forchheimer flow of Sisko Nanomaterial with Nonlinear thermal radiation by Lobatto III A technique, 2019, Article ID.8974572, 15 pages.

[5] M.U. Ahammad, M.H.Rashid , Md Obayedullah and Md. Harun-Ar-Rashid, Radiation Effect with Eckert number and Forchimer Number on Heat and Mass transfer over an Inclined plate in the influence of Suction/Injection flow. Vol.7(1),pp. 1-11, 2011.

[6] A.Majeed , A.Zeeshan, and F.M.Noori , Numerical study of Darcy Forchheimer model with activation energy subject to chemically reactive species and momentum slip of order two, Vol.9, pp.9,2019.

[7] K.Sreelakshmi,G.Sarojamma, O.D.Makinde,Dual stratification on the Darcy-Forchheimer flow of a Maxwell nanofluid over a stretching surface. Defect and Diffusion Forum, vol.387, (2018), pp. 207–217.

[8] Choi S.U.S, and Eastman JA, Enhancing thermal conductivity fluids with nanoparticles,American Society of Mechanical Engineering, Vol.231, 1995, pp.99-106.

[9] Habib-OlahSayehvandAmirBasiri Parsa, A new numerical method for investigation of thermophoresis and Brownian motion effects MHD nanofluid flow and heat transfer between parallel plates partially filled with porous medium. Results in Physics, Vol.7, 2017, pp.1595-1607.

[10] Rudraswamy N.G, and Gireesha B.J, Influence of chemical reaction and thermal radiation on MHD boundary layer flow and heat transfer of a nanofluid over an exponentially stretching sheet, Applied mathematics and physics, Vol.2, 2014, pp.24-32.

[11] Rashidi S, Akar S, and Bovand M, Volume of fluid model to simulate the nanofluid flow and entropy generation in asingle solar still,Vol.115, 2018, pp.400-410.

[12] Hayat T,Ijaz Khan M, and Waqas M, Numerical simulation for melting heat transfer and radiation effects in stagnation point flow of carbon-water nanofluid. Computer Methods, Vol.315, 2017, pp.1011-1024.

[13] Das K, Jana S, and Kunda P.K, Thermophoretic MHD slip flow over a permeable surface with variable fluid properties, Alexandria Engineering Journal, Vol.54, 2015, pp.35-44.

[14] Iftikhar Ahmed, Metib Alghamdi, Muhammad Amjad , Faisal Aziz, Tanvir Akbar and Taseer Muhammad , Numerical investigation of MHD flow of hyperbolic tangent nanofluid over a non-linear stretching sheet, Vol.9, 2023,https://doi.org/10.1016/j.heliyon.2023.e17658.

[15] Metib Alghamdi, Noreen Sher Akbar, Tayyab Zamir, Taseer Muhammad, Double layered combined convective heated flow of Eyring-Powell fluid across an elevated stretched cylinder using intelligent computing approach, Case Studies in Thermal Engineering, Vol 54, 2024.

[16] Noreen Sher Akbar, E.N. Maraj, Syed Irfan Shah, Taseer Muhammad, Nano particle distribution in blood via electroosmotic peristaltic flow in a non-uniform wavy membrane base capillaries, Sensors and Actuators A: Physical, vol 376, 2024.

[17] Noreen Sher Akbar, M. Fiaz Hussain, Taseer Muhammad, Metib Alghamdi, Thermal synthesize of shear thinning nanofluid in small flexible vessel type channel with low seepage Reynold number and Au nanoparticles, Case Studies in Thermal Engineering, vol 53, 2024.

[18] Noreen Sher Akbar, Javaria Akram, M. Fiaz Hussain, E.N. Maraj, Taseer Muhammad, Thermal storage study and enhancement of heat transfer through hybrid Jeffrey nanofluid flow in ducts under peristaltic motion with entropy generation, Thermal Science and Engineering Progress, vol 49, 2024

[19] Khalid Y. Ghailan, Noreen Sher Akbar, Ashwag Albakri, Mohammed M. Alshehri, Biological analysis of emerging nanoparticles with blood through propagating flow along a plumb porous canal in the occurrence of energy and heat transfer, Surfaces and Interfaces, vol 40, 2023.

[20] Anum Shafiq, Andaq Batur Colak, Tobassum Naz Sindhu, Significance of bioconvective flow of MHD thixotropic nanofluid passing through a vertical surface by machine learning algorithm, Chinese journal of physics, vol 80, 2022.

[21] Sidra Aman, Ilyas Khan, Zulkhibri Ismail, Mohd Zuki Salleh, Qasem M. Al-Mdallal, Heat transfer enhancement in free convection flow of CNTs Maxwell nanofluids with four different types of molecular liquids, Scientific reports, vol 7,2017

[22] Shafiq, Anum ,Mebarek-Oudina, Fateh Sindhu, Tabassum Naz , Abidi, Awatef, A study of dual stratification on stagnation point Walters' B nanofluid flow via radiative Riga plate: a statistical approach, The European Physical Journal Plus, Vol.136, Issue 4, article id.407.

[23] Rizwan Ul Haq, Feroz Ahmed Soomro, Toufik Mekkaoui and Qasem Al-Mdallal, MHD natural convection flow enclosure in a corrugated cavity filled with a porous medium, Heat and Mass Transfer , Vol. 121:1168-1178.

[24] Anum Shafiq, Andaç Batur Çolak, and abassum Naz Sindhu, A Hybrid Approach of Buongiorno's Law and Darcy–Forchheimer Theory Using Artificial Neural Networks: Modeling Convective Transport in Al2O3-EO Mono-Nanofluid Around a Riga Wedge in Porous Medium, International Journal of numerical research, ISSN:0271-2091.

[25] Shafiq, Anum ;Çolak, Andaç Batur ; and Sindhu, Tabassum Naz, Modeling of Darcy-Forchheimer magnetohydrodynamic Williamson nanofluid flow towards nonlinear radiative stretching surface using artificial neural network, nternational Journal for Numerical Methods in Fluids, vol. 95, issue 9, pp. 1502-1520.